in-Aid for Scientific Research from the Ministry of Education, Science and Culture of Japan.

Registry No. 1, 123464-24-4; 2, 20834-12-2; 3, 123464-25-5; 4, 123464-26-6; 5, 123464-27-7; 6, 123464-28-8; 7, 123464-29-9; 8, 40299-68-1; 9, 123464-30-2; 10, 123464-31-3; 11, 74629-13-3; 12, 123464-32-4; 13, 123464-33-5; 3-*O*-benzyl-*sn*-glycerol, 56552-80-8.

Supplementary Material Available: Optical rotations, physical states, melting points, and IR and ^{1}H NMR spectral data for compounds 1-13 (4 pages). Ordering information is given on any current masthead page.

Conformation of the Phosphate-Methylated DNA Dinucleotides d(CpC) and d(TpC). Formation of a Parallel Miniduplex Exclusively for the *S* Configuration at Phosphorus

Peter J. L. M. Quaedflieg,* Niek L. H. L. Broeders, Leo H. Koole, Marcel H. P. van Genderen, and Henk M. Buck

Department of Organic Chemistry, Eindhoven University of Technology, P.O. Box 513, 5600 MB Eindhoven, The Netherlands

Received April 19, 1989

It has been shown that the phosphate-methylated DNA dinucleotides d(CpC) (1) and d(TpC) (2) form a parallel miniduplex exclusively for the *S* configuration on phosphorus, which corresponds with outward orientation of the methyl group from the helix into the solvent. The melting temperatures (T_m values) of the parallel duplexes of (S_P)-1 and (S_P)-2 are 33 °C and 26 °C, respectively. The phosphate-sugar backbone strands adopt a standard right-handed geometry. The imino resonances in the 600-MHz ^{1}H NMR spectra strongly point at C-C base pairing via two symmetry-related NH_2···N hydrogen bonds, as was also observed in the X-ray crystal structure of 2'-deoxycytidine. From our previous work, it is known that phosphate-methylated d(TpT) forms parallel miniduplexes with an equal stability for the S_P and R_P diastereoisomers. Therefore, it is concluded that the R_P configuration (which is associated with location of the methyl group inside the helix groove) is unfavorable in the case of C-C base pairing. This conclusion was corroborated by AMBER molecular mechanics calculations, which showed that the larger propeller twist angle for C-C base pairing (≈41°), in comparison with T-T base pairing (≈25°), results in narrowing of the helix groove.

Introduction

Methylation of the phosphate groups in d(T_n) DNA oligomers (n = 2-8) results in the formation of a double helix with T-T base pairs and *parallel* orientation of the backbone strands.[1] In our previous work, we have focussed on the stability and molecular structure of these parallel duplexes.[1,2] In studying the stability, it was found that the T_m values rise linearly with increasing duplex length. This is explained by the lack of electrostatic phosphate-phosphate repulsion, i.e., elongation of the backbone strands leads to an increased stability since hydrogen bonding and base stacking are increased without the introduction of repulsive forces.[3] Our structural model was based on experimental data (i.e., X-ray crystal structure of 3',5'-di-*O*-acetylthymidine,[1,4] detailed ^{1}H NMR investigations of phosphate-methylated d(TpT)$_2$ in stereochemically pure form, imino proton chemical shifts for longer systems), as well as on AMBER molecular mechanics calculations.[2] This led to a symmetrical parallel duplex structure with a relatively small helix diameter (16 Å vs 21 Å for Watson-Crick B DNA), right-handed backbone strands, and 8 base pairs per full turn. Molecular models showed that the parallel duplex can easily accommodate the methyl groups, both for the S_P configuration (methyl pointing away from the duplex) and the R_P configuration (methyl located inside the helix groove).[2] Thus, the different configurations of the methylated phosphate groups in the backbone have no impact on the stability of the duplex. This readily explains why well-defined sharp melting transitions were observed for all parallel T-T duplexes.[3]

We have subsequently addressed the question of whether parallel duplex formation is restricted to T-T base pairing. The X-ray crystal structures of 2'-deoxy-3',5'-di-*O*-acetyladenosine[5a] and 2'-deoxy-3',5'-di-*O*-acetylguanosine[5b] showed highly complex hydrogen-bonded networks, from which we concluded that parallel A-A or G-G base pairing is rather unlikely. Thus, we focussed on dC structures, for which it was known from literature that parallel C-C base pairing can occur. For example, the X-ray crystal structure of 2'-deoxycytosine shows parallel C-C base pairing in which the two C bases are linked via two identical NH_2···N hydrogen bonds.[6] These data prompted us to synthesize the phosphate-methylated dinucleotides d(CpC) (1) and d(TpC) (2) in stereochemically pure form and to investigate possible duplex formation in these structures.[7] In this paper we describe a conformational study of the R_P and S_P diastereoisomers of 1 and 2, on the basis of variable-temperature high-field NMR and

(1) (a) Koole, L. H.; van Genderen, M. H. P.; Frankena, H.; Kocken, H. J. M.; Kanters, J. A.; Buck, H. M. *Proc. K. Ned. Akad. Wet., Ser. B* **1986**, *89*, 51. (b) Koole, L. H.; van Genderen, M. H. P.; Buck, H. M. *J. Am. Chem. Soc.* **1987**, *109*, 3916.

(2) (a) van Genderen, M. H. P.; Koole, L. H.; Aagaard, O. M.; van Lare, C. E. J.; Buck, H. M. *Biopolymers* **1987**, *26*, 1447. (b) van Genderen, M. H. P.; Koole, L. H.; Buck, H. M. *Recl. Trav. Chim. Pays-Bas* **1989**, *108*, 28.

(3) van Genderen, M. H. P.; Koole, L. H.; Merck, K. B.; Meijer, E. M.; Sluyterman, L. A. AE.; Buck, H. M. *Proc. K. Ned. Akad. Wet., Ser. B* **1987**, *90*, 155.

(4) Wilson, C. C.; Low, J. N.; Tollin, P.; Wilson, H. R. *Acta Crystallogr., Sect. C: Cryst. Struct.* **1986**, *42*, 584.

(5) (a) Koole, L. H.; Buck, H. M.; Kanters, J. A.; Schouten, A. *Can. J. Chem.* **1987**, *65*, 326. (b) Koole, L. H.; Buck, H. M.; Kanters, J. A.; Schouten, A. *Ibid.* **1988**, *66*, 2634.

(6) Young, D. W.; Wilson, H. R. *Acta Crystallogr., Sect. B.: Struct. Sci.* **1975**, *31*, 961.

(7) Preliminary results on 1 have been published: Koole, L. H.; Broeders, N. L. H. L.; van Genderen, M. H. P.; Quaedflieg, P. J. L. M.; van der Wal, S.; Buck, H. M. *Proc. K. Ned. Akad. Wet., Ser. B.* **1988**, *91*, 245.

0022-3263/90/1955-0122$02.50/0

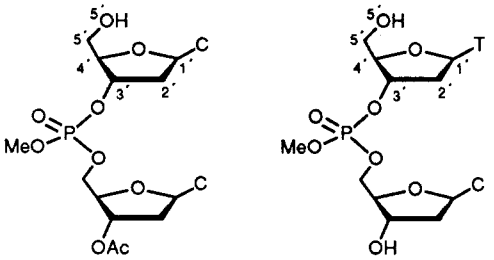

1 2

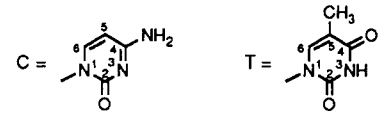

UV hyperchromicity experiments. Furthermore, the preparation of phosphate-methylated d(TpC) in stereochemically pure form is described (synthesis of (R_P)-1 and (S_P)-1 was reported previously by us).[8] It is found that (S_P)-1 and (S_P)-2 show duplex formation, whereas (R_P)-1 and (R_P)-2 are present only in the single strand form. These data show for the first time that chirality on the backbone phosphate groups in parallel DNA duplexes can affect the stability of the duplex.

Results and Discussion

The full set of vicinal $^1H-^1H$ and $^1H-^{31}P$ coupling constants measured at 600 MHz[9] for the R_P and S_P diastereoisomers of 1 and 2 in D_2O is given in Table I. These data can be used to determine the conformational properties of the individual 2'-deoxyribose units and the backbone bonds γ ($C_{4'}-C_{5'}$) and β ($C_{5'}-O_{5'}$).[10] The 2'-deoxyribose units are involved in a rapid conformational equilibrium between a $C_{3'}$-endo and a $C_{2'}$-endo puckered form.[11] The conformation around the γ bond can be best described as a rapid equilibrium over the staggered rotamers γ^+, γ^t, and γ^-.[12] Analogously, the β conformation is described in terms of a rapid equilibrium over β^+, β^t, and β^-.[13]

The conformational data on R_P and S_P 1 and 2 are summarized in Table II. Clearly, all four systems adopt a highly similar sugar-backbone conformation in solution. The 2'-deoxyribose rings are predominantly in the $C_{2'}$-endo form, while the γ and β bonds are in the γ^+ and β^t conformations, respectively. Thus, a standard right-handed conformation is found for all four structures.

In order to investigate possible duplex formation in our systems, we performed variable-temperature ^1H NMR experiments in which we particularly focussed on the chemical shifts of the nonexchangeable base protons (i.e., H_5 and H_6 of C, H_6 and 5-CH_3 of T). The chemical shifts of these protons are known to be sensitive to changes in base stacking, which are associated with a duplex $\rightleftarrows$ single strand melting transition.[15] Figure 1 shows the $\delta(H_6)$ vs temperature profiles measured for 1 (R_P and S_P). Both cytidine H_6 protons in (S_P)-1 show a sigmoidal δ vs temperature curve, whereas continuously decreasing profiles are found for the R_P diastereoisomer. The midpoint of the sigmoidal curves of (S_P)-1 is at approximately 33 °C (vide infra). Analogous experiments were performed for 2 (R_P and S_P); the δ vs temperature profiles of H_6(T) and H_6(C) are shown in Figure 2. Again, a sigmoidally shaped δ vs temperature curve is found exclusively for (S_P)-2 (midpoint approximately 26 °C). The downfield shift of H_6 during the melting process is typical for pyrimidine–pyrimidine base stacking, as was reported by Cheng and Sarma[16] in their studies on natural, single-stranded dinucleotides. In contrast to purine–pyrimidine or purine–purine stacking, the H_6 proton of a pyrimidine resides in a deshielding region when stacked with another pyrimidine base, as is evident from chemical shift calculations.[17]

Additional evidence for exclusive base–base association of the S_P diastereoisomers of 1 and 2 and not for the R_P counterparts could be inferred from UV hyperchromicity experiments. This technique is based on the fact that nucleotide bases in the destacked form correspond to an enlarged UV extinction if compared to the stacked situa-

(8) Koole, L. H.; Moody, H. M.; Broeders, N. L. H. L.; Quaedflieg, P. J. L. M.; Kuijpers, W. H. A.; van Genderen, M. H. P.; Coenen, A. J. J. M.; van der Wal, S.; Buck, H. M. *J. Org. Chem.* **1989**, *54*, 1657.

(9) ^1H NMR (600 MHz) spectra were measured on the Bruker AM 600 NMR spectrometer of the Dutch National hf NMR facility at Nijmegen, The Netherlands.

(10) See, for instance: (a) Altona, C. *Recl. Trav. Chim. Pays-Bas* **1982**, *101*, 413. (b) Koole, L. H.; van Genderen, M. H. P.; Buck, H. M. *J. Org. Chem.* **1988**, *53*, 5266. (c) Haasnoot, C. A. G.; de Leeuw, F. A. A. M.; Altona, C. *Tetrahedron* **1980**, *36*, 2783. (d) Lankhorst, P. P.; Haasnoot, C. A. G.; Erkelens, C.; Altona, C. *J. Biomol. Struct. Dyns.* **1984**, *1*, 1387.

(11) The $C_{2'}$-endo and $C_{3'}$-endo puckered conformations of the 2'-deoxyribose ring can be drawn as follows:

The standard right-handed B DNA structure (Watson–Crick model) corresponds with $C_{2'}$-endo puckered sugar rings in each nucleotide unit.

(12) The Newman projections of the staggered rotamers around the $C_{4'}-C_{5'}$ bond are defined as follows:

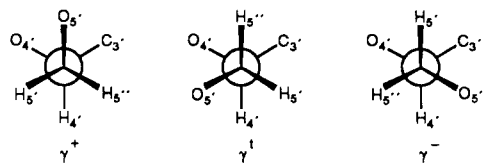

The standard right-handed B DNA conformation (Watson–Crick model) corresponds with γ^+ conformation in all nucleotides.

(13) The Newman projections of the staggered rotamers around the $C_{5'}-O_{5'}$ bond are defined as

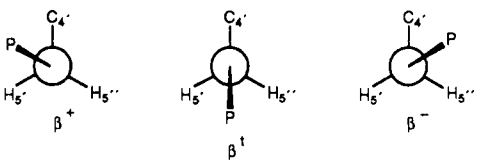

For all DNA structures, the β^t rotamer has the highest population density.

(14) The time-averaged population of the $C_{2'}$-endo conformation was calculated from the coupling constants $J_{1'2''}$ and $J_{2''3'}$, according to the formula: $x(C_{2'}\text{-endo}) = (17.8 - J_{1'2''} - J_{2''3'})/10.9$ (see ref 10a). The population distribution over the $C_{4'}-C_{5'}$ rotamers was solved from the equations:

$$J_{4'5'(5'')}(\text{exp}) = x(\gamma^+)\cdot J_{4'5'(5'')}(\gamma^+) + x(\gamma^t)\cdot J_{4'5'(5'')}(\gamma^t) + x(\gamma^-)\cdot J_{4'5'(5'')}(\gamma^-)$$

along with $x(\gamma^+) + x(\gamma^t) + x(\gamma^-) = 1$. We used the $J_{4'5'(5'')}$ values for the individual γ rotamers, as proposed by Haasnoot et al. (ref 10c), i.e., $J_{4'5'}(\gamma^+) = 2.4$ Hz, $J_{4'5'}(\gamma^t) = 2.6$ Hz, $J_{4'5'}(\gamma^-) = 10.6$ Hz, $J_{4'5''}(\gamma^+) = 1.3$ Hz, $J_{4'5''}(\gamma^t) = 10.5$ Hz, $J_{4'5''}(\gamma^-) = 3.8$ Hz. In order to obtain the population distribution over the $C_{5'}-O_{5'}$ rotamers, we solved the set of equations

$$J_{P5'(5'')}(\text{exp}) = x(\beta^+)\cdot J_{P5'(5'')}(\beta^+) + x(\beta^t)\cdot J_{P5'(5'')}(\beta^t) + x(\beta^-)\cdot J_{P5'(5'')}(\beta^-)$$

along with $x(\beta^+) + x(\beta^t) + x(\beta^-) = 1$. For the coupling constants in the individual β rotamers we used the values as proposed by Lankhorst et al. (ref 10d), i.e., $J_{P5'}(\beta^+) = J_{P5'}(\beta^t) = J_{P5''}(\beta^t) = J_{P5''}(\beta^-) = 2.4$ Hz, $J_{P5'}(\beta^-) = J_{P5''}(\beta^+) = 23.0$ Hz.

(15) Patel, D. In *Nucleic Acid Geometry and Dynamics*; Sarma, R. H., Ed.; Pergamon Press: New York, 1980.

(16) Cheng, M. D.; Sarma, R. H. *J. Am. Chem. Soc.* **1977**, *99*, 7333.

(17) (a) Giessner-Prettre, C.; Pullman, B. *Biopolymers* **1976**, *15*, 2277. (b) Prado, F. R.; Giessner-Prettre, C. *J. Mol. Struct. Theochem.* **1981**, *76*, 81.

Table I. ^1H–^1H and ^{31}P–^1H NMR Coupling Constants (in Hz), Measured for S_P and R_P Phosphate-Methylated d(CpC) and d(TpC) in D_2O at 20 °C

	(S_P)-d(CpC)[a]		(R_P)-d(CpC)[b]		(S_P)-d(TpC)[c]		(R_P)-d(TpC)[d]	
coupling constant	dCp	pdC	dCp	pdC	dTp	pdC	dTp	pdC
$J_{1'2'}$	8.0	7.4	7.6	7.2	6.1	6.7	6.1	6.7
$J_{1'2''}$	6.0	6.2	6.0	6.4	6.1	6.7	6.1	6.7
$J_{2'3'}$	7.2	7.2	7.2	7.2	6.7	6.7	6.7	6.7
$J_{2''3'}$	2.6	3.1	3.0	3.0	2.4	4.9	2.4	5.1
$J_{2'2''}$	−14.8	−14.6	−14.4	−14.8	−14.6	−14.0	−14.7	−13.4
$J_{3'P}$	4.8		4.0		3.7		2.7	
$J_{3'4'}$	3.2	2.3	4.0	3.0	2.4	2.7	5.2	3.1
$J_{4'5'}$	4.0	2.2[e]	3.6	1.8[e]	4.9	2.8	4.3	2.4
$J_{4'5''}$	4.0	3.0[e]	3.6	4.2[e]	4.9	5.5	4.3	5.5
$J_{5'P}$		5.0[e]		6.3[e]		6.1		5.5
$J_{5''P}$		7.2[e]		5.9[e]		5.5		5.5
$J_{5'5''}$	−12.4	−11.0	−12.4	−10.9	−12.5	−12.0	−12.5	−11.6

[a] Measured at a DNA single-strand concentration of 11.7 mM. [b] Measured at a DNA single-strand concentration of 3.7 mM. [c] Measured at a DNA single-strand concentration of 8.0 mM. [d] Measured at a DNA single-strand concentration of 4.6 mM. [e] Obtained by iterative computer simulation of the non-first-order pattern of $H_{4'}/H_{5'}/H_{5''}$.

Table II. Calculated Time-Averaged Populations of the $C_{2'}$-endo Puckered Ring Form of the 2'-Deoxyribose Rings, the $C_{4'}$–$C_{5'}$ (γ) Rotamers, and the $C_{5'}$–$O_{5'}$ (β) Rotamers[14]

	(S_P)-d(CpC)		(R_P)-d(CpC)		(S_P)-d(TpC)		(R_P)-d(TpC)	
	dCp	pdC	dCp	pdC	dTp	pdC	dTp	pdC
$x(C_{2'}\text{-endo})$	0.84	0.78	0.81	0.77	0.85	0.57	0.85	0.55
$x(\gamma^+)$	0.57	0.82	0.65	0.69	0.39	0.52	0.51	0.54
$x(\gamma^t)$	0.24	0.18	0.21	0.31	0.31	0.45	0.27	0.46
$x(\gamma^-)$	0.19	0.00	0.14	0.00	0.30	0.03	0.22	0.00
$x(\beta^+)$		0.23		0.17		0.15		0.15
$x(\beta^t)$		0.64		0.64		0.67		0.70
$x(\beta^-)$		0.13		0.19		0.18		0.15

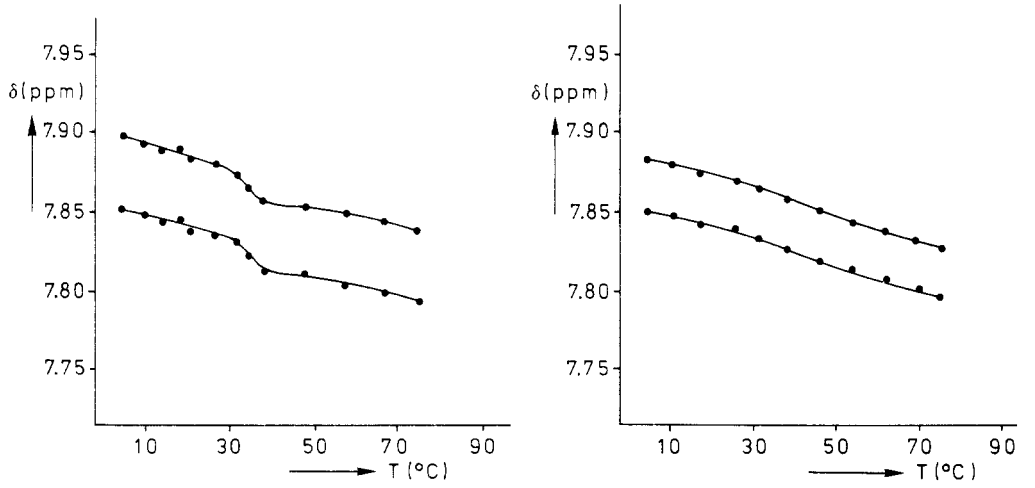

Figure 1. ^1H NMR chemical shift vs temperature profiles in D_2O of the H_6 protons of (S_P)-d(CpC) (left) and (R_P)-d(CpC) (right). For both diastereoisomers, the upper profile corresponds with the dCp residue and the lower profile with the pdC residue.

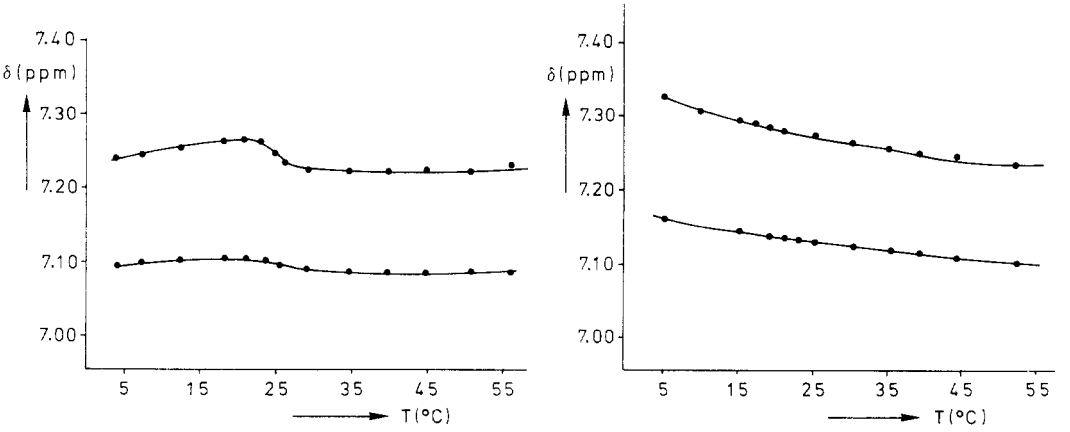

Figure 2. ^1H NMR chemical shift vs temperature profiles in D_2O of the H_6 protons of (S_P)-d(TpC) (left) and (R_P)-d(TpC) (right). For both diastereoisomers, the upper profile corresponds with the pdC residue and the lower profile with the dTp residue.

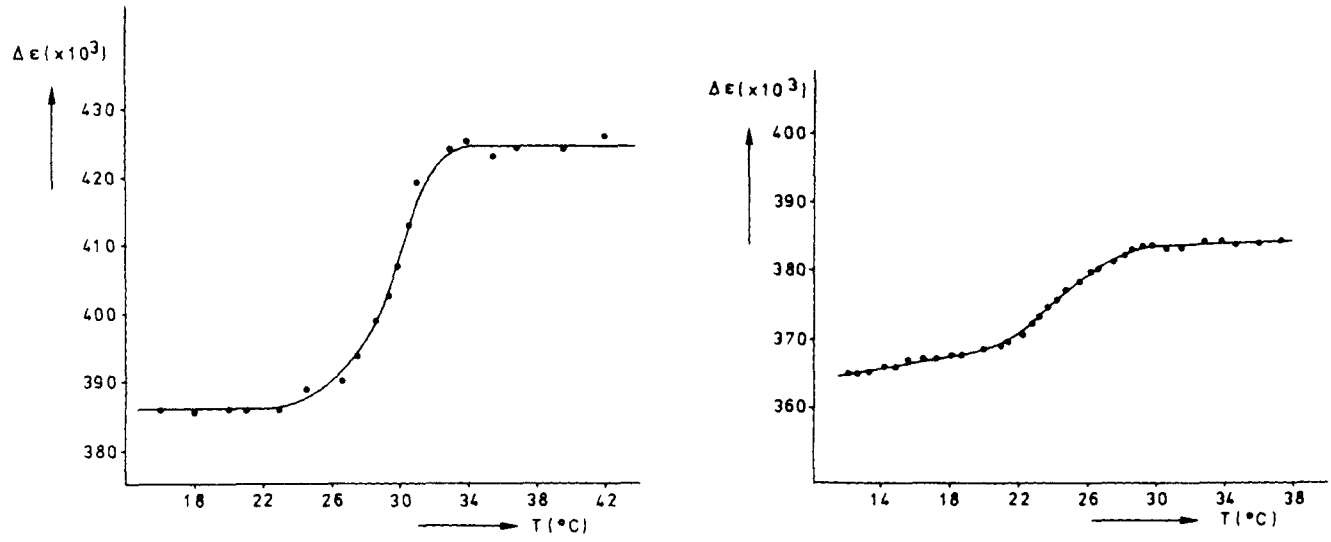

Figure 3. Left: UV extinction vs temperature profile for (S_P)-d(CpC) at a concentration of 6.1 μM (T_m value 29.5 °C). Right: UV extinction vs temperature profile for (S_P)-d(TpC) at a concentration of 5.9 μM (T_m value 24.6 °C).

tion. Thus, a temperature-induced melting transition is reflected into a UV hyperchromicity effect.[18] The ϵ vs temperature profiles were clearly consistent with the NMR data: sigmoidal melting curves were found for (S_P)-**1** and (S_P)-**2** and not for the R_P diastereoisomers (Figure 3).

Using the thermodynamic equations as derived by Marky and Breslauer,[19] we extracted the ratio $\Delta H_d/(n + 1)$ (ΔH_d = van't Hoff dissociation enthalpy, n = number of strands that associate to form an n-mer complex) from the sigmoidal melting curves. This was done by careful determination of the first derivative of the f (fraction of single strands) vs temperature plot at the T_m value (slope = $\Delta H_d/(2 + 2n)RT_m^2$).[19,20] For (S_P)-**1** and (S_P)-**2**, values of 282 and 246 kJ/mol were found for $\Delta H_d/(n + 1)$, respectively.

In addition, we used the UV hyperchromicity technique to monitor the T_m value as a function of the total strand concentration (C_T) of (S_P)-**1** and (S_P)-**2**. For (S_P)-**1** it was found that increasing C_T from 1.5 to 6.1 μM results in a T_m increase from 28.3 to 29.5 °C. Similarly, increasing C_T for (S_P)-**2** from 1.7 to 10.8 μM results in a T_m increase from 23.2 to 25.1 °C.[20] The experimental data were used to construct a plot of $1/T_m$ vs ln C_T. Figure 4 shows the $1/T_m$ vs ln C_T plot as measured for (S_P)-**2**. According to the Breslauer model, the slope of such a plot equals $-(n - 1)R/\Delta H_d$, i.e., a second relationship between ΔH_d and n is obtained in this way. The ratio $(n - 1)/\Delta H_d$ was found to be 1.13×10^{-3} and 1.55×10^{-3} mol/kJ for (S_P)-**1** and (S_P)-**2**, respectively. Solution of n and ΔH_d resulted in the following: (S_P)-**1**, n = 1.94 and ΔH_d = 829 kJ/mol; (S_P)-**2**, n = 2.23 and ΔH_d = 793 kJ/mol. These data clearly show that *dimeric* structures are formed. The van't Hoff enthalpies of dissociation are surprisingly high, which may be attributed to the absence of electrostatic phosphate–phosphate repulsion, as well as to the unusual mode of base–base stacking that is present in the parallel duplexes of (S_P)-**1** and (S_P)-**2**.

In order to set up a structural model of the duplexes of (S_P)-**1** and (S_P)-**2**, it is important to realize that the observation of single degenerate ^{1}H NMR spectra for (S_P)-**1**

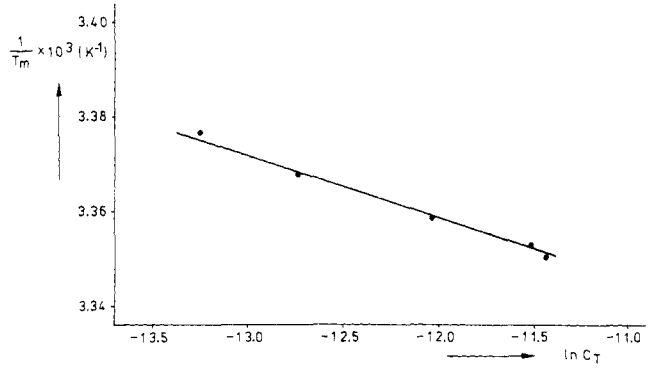

Figure 4. Plot of $1/T_m$ vs ln C_T as measured for (S_P)-**2**. T_m values were determined by computer fitting of the melting profiles with a sigmoidal curve. C_T values were obtained from UV extinction measurements.

and (S_P)-**2** proves that the strands are symmetry related. Combining this information with the result that a *duplex* is formed, it can be concluded that parallel C–C base pairing occurs (along with parallel T–T base pairing in the case of (S_P)-**2**). In the case of antiparallel base pairing, far more complex ^{1}H NMR spectra would have been obtained since the coupled nucleotides then reside in different magnetic environments. The present data are consistent only with parallel C–C and parallel T–T base pairing as encountered in the X-ray crystal structures of 2′-deoxycytidine[6] and 3′,5′-di-*O*-acetylthymidine[1] (vide supra). In order to verify the presence of this type of base pairing in (S_P)-**1** and (S_P)-**2**, we focussed on the low-field regions of the ^{1}H NMR spectra of these systems in H_2O/D_2O (80/20 v/v). An amino proton resonance was found at δ 8.93 for (S_P)-**1** at a sample temperature of 4 °C and a DNA concentration of 11.7 mM. This strongly indicates formation of NH_2···N hydrogen bonds.[21] It should be noted that in fact two distinct amino proton resonances are expected in this spectral region, each corresponding to one of the C–C base pairs in (S_P)-**1**.[22]

(18) (a) Saenger, W. In *Principles of Nucleic Acid Structure*; Springer-Verlag: New York, 1984; pp 141–149. (b) Porschke, D. *Biopolymers* **1971**, *10*, 1989.
(19) Marky, L. A.; Breslauer, J. *Biopolymers* **1987**, *26*, 1601.
(20) T_m values and first derivatives were determined by computer-aided fitting of the melting profiles into sigmoidal curves.
(21) Wüthrich, K. In *NMR of Proteins and Nucleic Acids*; Wiley and Sons: New York, 1986.
(22) It should be noted that the two amino protons that are involved in base pairing within the same C–C base pair are symmetry-related, i.e., they are in the same magnetic environment. Therefore, only two amino resonances are expected for the duplex of (S_P)-**1**, one for the C–C base pair at the 5′ end and one for the C–C base pair at the 3′ end.

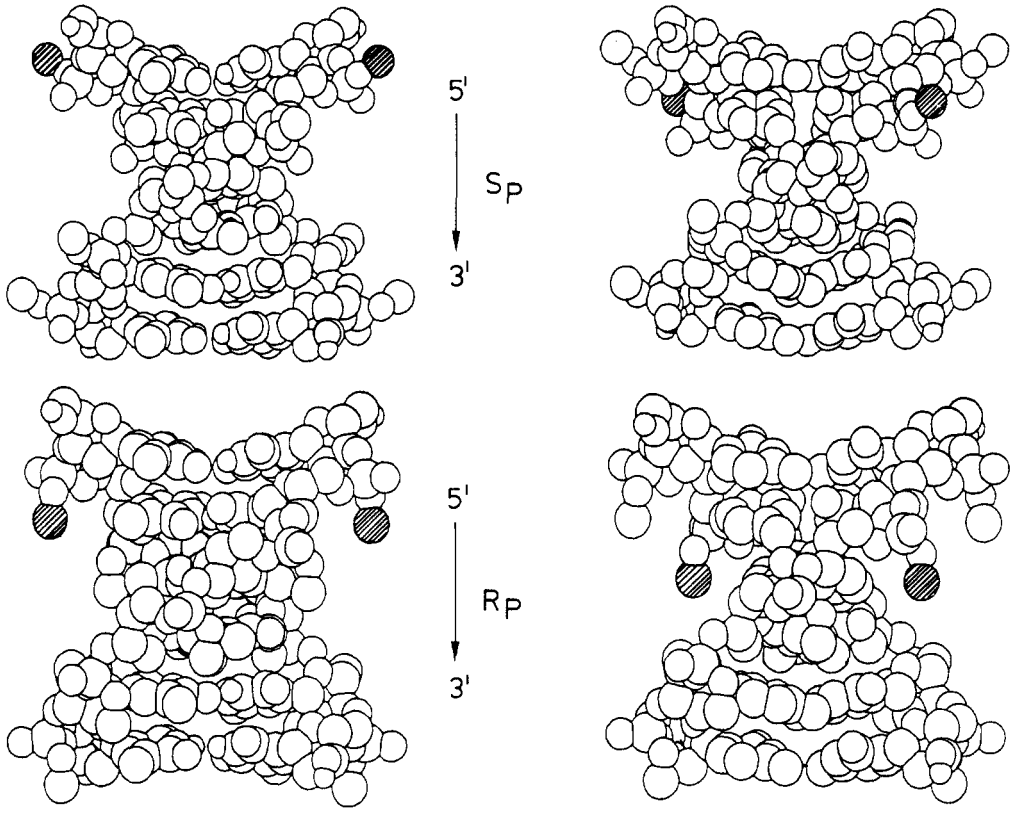

Figure 5. Structural models of the parallel duplexes of S_P and R_P phosphate-methylated d(T_6) (left) and d(C_6) (right), as obtained from AMBER molecular mechanics calculations. The methyl groups of the phosphates have been shaded. Note that the methyl groups are forced into the helix groove in the case of C–C base pairing and R_P configuration (bottom-right drawing). In the three other cases, the methyl groups are easily accommodated.

Apparently, broadening of these signals (the observed line width at half height at 4 °C is 30 Hz) prevents their resolution. Increasing the sample temperature leads to further broadening and upfield shifting of the single peak, which eventually disappears above 30 °C. This effect corresponds to gradual disruption of the hydrogen bonds leading to increased exchange with the protons of the solvent. For (S_P)-**2** in H_2O/D_2O (80/20 v/v) at 4 °C and a DNA concentration of 8.0 mM, two distinct proton resonances appeared; one at δ 13.05[1] and one at δ 9.02. These δ values clearly indicate the presence of a parallel T–T base pair (δ of the two symmetry-related imino protons, 13.05), along with a parallel C–C base pair (δ of the amino protons, 9.02, vide supra). Both signals also broadened upon increasing the sample temperature; they could not be observed for temperatures higher than approximately 20 °C.

Finally, two important remarks should be made. The first one is that a different type of parallel C–C base pairing has been reported previously for natural d(CTCTCT) under strongly acidic conditions.[23] More specifically, these data refer to C^+–C base pairing, i.e., one of the cytosines is protonated. Duplex formation on the basis of C^+–C base pairing can be safely excluded for our systems, since: (i) no proton resonance was found at δ = 11.1 ppm, which is typical for the imino proton in the C^+–C base pair;[23] (ii) our experiments were performed at neutral pH (pH between 7.0 and 7.5), while C^+–C base pairing has been observed only at much lower pH values (pK_a of cytosine = 4.6); (iii) for (S_P)-**2**, we have observed C–C base pairing along with T–T base pairing, while C^+–C base pairing as reported by Sarma et al. is associated with thymine–thymine bulges.[23]

The second remark concerns the fact that one- and two-dimensional nuclear Overhauser NMR spectroscopy can hardly be used for structural analysis of our systems.[24] This is the result of the inherent symmetry of the parallel duplexes of (S_P)-**1** and (S_P)-**2**, which implies that every interstrand NOE is overlapped by a stronger intrastrand NOE peak.[1] Apart from this, it is clear that the dimer duplexes of (S_P)-**1** and (S_P)-**2** are borderline cases to observe either positive or negative NOE effects, i.e., application of NOE techniques is hampered by the fact that the resulting intensities of NOE contacts are very low.[25]

Concluding Remarks

We have shown in this work that formation of parallel DNA duplex structures upon methylation of the backbone phosphate groups may involve C–C and/or T–T base pairs. However, C–C base pairing leads to a parallel duplex *only in the case of the* S_P configuration on phosphorus, i.e., for outward orientation of the methyl group from the helix into the solvent bulk. Obviously, the inward location of the methyl group (R_P configuration), which is easily accommodated in the case of T–T parallel DNA, is unfavorable for C–C parallel DNA. Molecular modeling studies have revealed that a larger propeller twist angle in the C–C base pair (≈41°), as compared to the T–T base pair (≈25°), is responsible for this stereochemical selection.[26] The

(23) Sarma, M. H.; Gupta, G.; Sarma, R. H. *FEBS Lett.* **1986**, *205*, 223.

(24) One-dimensional NOE could be used to determine the orientation of the C bases in (S_P)-**1**. For both the dCp and pdC residues, it was found that the NOE effect on H_6 was negligible upon saturation of $H_{1'}$, whereas saturation of $H_{2'}$ (increase 12% for dCp and 14% for pdC) and $H_{3'}$ (increase 6% for dCp and pdC) clearly led to NOE effects. It follows therefore that H_6 is located on the endo side of the 2′-deoxyribose ring, so the C bases reside in the standard anti conformation.

(25) Derome, A. E. In *Modern NMR Techniques for Chemistry Research*; Pergamon Press: Oxford UK, 1987; pp 98–127.

larger propeller twist angle for C–C base pairing results in narrowing of the helix groove, which can then no longer accommodate the methyl group in the case of the R_P configuration (see Figure 5). It may of interest to note that we have found in our previous work[1b] that the phosphate-methylated dodecamer d(CpCpCpCpCpCpTpTpTpTpTpT) does not show duplex formation. From the present results, it can now be concluded that this is due to the fact that the dodecamer exists as a random mixture of R_P and S_P phosphate-methylated d(CpC) units.

The present results show for the first time that formation of parallel DNA duplexes is not simply a matter of shielding of the phosphate–phosphate electrostatic repulsions alone. It seems to us that the way of accommodation of the methyl groups for both possible configurations on phosphorus together with elimination of phosphate–phosphate repulsions between both strands are decisive with respect to formation of a parallel DNA duplex.

Experimental Section

Materials and Methods. The ^{1}H NMR spectra were recorded on a Bruker AM 600[9] or a CXP 300 NMR spectrometer. Tetramethylsilane (TMS) was used as the internal standard for samples in organic solvents. For samples in aqueous solution (either D_2O or H_2O/D_2O 80/20), tetramethylammonium bromide (δ 3.18) was used as the standard. During the experiments, the residual HDO peak was suppressed with the method of Haasnoot et al.[27] Coupling constants were taken from the expansions of the 600-MHz ^{1}H NMR spectra. ^{31}P NMR spectra were recorded on a Bruker AC 200 spectrometer at a frequency of 80.9 MHz. The ^{31}P NMR chemical shifts were related to an 85% H_3PO_4 solution (δ = 0 ppm), while shifts are designated positive downfield of this reference. UV hyperchromicity experiments were performed on a Perkin-Elmer 124 spectrophotometer at a wavelength of 260 nm. All samples were dissolved in aqueous TrisHCl buffer solutions of pH 7.5. For all routine chromatographic separations, we used ICN Biochemicals TSC 60 A silica gel. Pyridine was distilled from KOH pellets and stored on 4-Å molecular sieves. 1*H*-Tetrazole was purified through sublimation. *tert*-Butyl hydroperoxide was used as received (75% solution in di-*tert*-butyl peroxide). Reactions were routinely run in an atmosphere of dry nitrogen or dry argon. Prior to each reaction step, we removed last traces of water by coevaporation with small portions of dry pyridine. Unless otherwise stated, reactions were run at ambient temperature. The separation of the diastereoisomers was developed on a HP 1090 gradient HPLC system. Preparative chromatography was executed on a HPLC system consisting of a Waters M 590 solvent delivery system equipped with a solvent select valve module, an Alltech RSil C18 10-μm column (250 × 22 mm), and a Waters 480 detector. The chromatographic parameters as previously reported by Stec et al.[28] were slightly modified. Separation was performed at pH 4.2; estimated values of K'_{R_p} and α are 2.8 and 1.07, respectively. Acetonitrile (12%) was used as a modifier. The purity of all title compounds was judged to be >95% by HPLC, ^{1}H NMR, and ^{31}P NMR determinations.

Synthesis of Phosphate-Methylated d(TpC). Thymidine (5.0 g, 20.7 mmol) was dissolved in 50 mL of dry pyridine, and 4-monomethoxytrityl chloride (7.65 g, 24.8 mmol) was added. The solution was stirred overnight in the darkness. After evaporation of the pyridine, the residue was coevaporated with toluene and then recrystallized from toluene. Filtration and drying at 50 °C yielded 5′-*O*-(4-monomethoxytrityl)thymidine as a white solid (9.97 g, 94%), mp 102–104 °C.[29] Anal. Calcd: C, 70.04; H, 5.84; N, 5.46. Found: C, 70.30; H, 5.48; N, 5.13. ^{1}H NMR ($CDCl_3$): δ 1.45 (3 H, s, CH_3 base), 2.41 (1 H, m, $H_{2''}$), 2.88 (1 H, m, $H_{2'}$), 3.41 (2 H, m, $H_{5'/5''}$), 3.78 (3 H, s, OCH_3), 4.07 (1 H, m $H_{4'}$), 4,58 (1 H, m, $H_{3'}$), 6.43 (1 H, t, $H_{1'}$, J = 6 Hz), 6.85 (2 H, d, trityl, J = 8 Hz), 7.12–7.49 (12 H, m, trityl), 7.58 (1 H, s, H_6), 9.24 (1 H, s, NH).

5′-*O*-(4-Monomethoxytrityl)thymidine (6.18 g, 12.0 mmol) and 1*H*-tetrazole (0.42 g, 6.0 mmol) were dissolved in 60 mL of dry pyridine. Bis(*N*,*N*-diisopropylamino)methoxyphosphine[8] (3.78 g, 14.4 mmol) was added, and the reaction mixture was stirred for 30 min. Complete formation of the desired phosphoramidite was seen in the ^{31}P NMR spectrum ($CDCl_3$: δ 149.8 and 149.1). Then, a solution of 2′-deoxycytidine (3.00 g, 13.2 mmol) and 1*H*-tetrazole (2.31 g, 33.0 mmol) in 30 mL of dry pyridine was added, and the mixture was stirred for 1 h. ^{31}P NMR showed complete consumption of the phosphoramidite, which had fused almost exclusively with the 5′-OH of the 2′-deoxycytidine[30] ($CDCl_3$: δ 141.2 and 140.9). The phosphite was oxidized with 7 mL of *tert*-butyl hydroperoxide in 10 min. After evaporation of all volatiles and coevaporation with toluene, the residue was chromatographed on a silica gel column with dichloromethane/methanol (9:1 v/v) as eluent (R_f = 0.22). The phosphate was obtained in a yield of 53% (5.2 g). ^{31}P NMR ($CDCl_3$): δ −0.02 and −0.04.

The 4-monomethoxytrityl group was removed by dissolving the phosphate (1.09 g, 1.33 mmol) in 40 mL of an acetic acid/water (4:1 v/v) mixture and stirring the mixture overnight. After evaporation of all volatile matters, the residue was taken up in 60 mL of water and washed three times with diethyl ether. The aqueous layer was concentrated, and the residual gum was subjected to reversed-phase HPLC.[8] Assignment of the different configurations at phosphorus was performed as described in ref 8.

S_P Diastereoisomer (20 °C, 8.0 mM). ^{31}P NMR (D_2O): δ 2.01. ^{1}H NMR (D_2O): δ 2.38 (3 H, s, CH_3 base), 2.77 (1 H, m, $H_{2'}$, pdC), 2.84 (1 H, m, $H_{2'}$ dTp), 2.85 (1 H, m, $H_{2''}$ pdC), 2.95 (1 H, m, $H_{2''}$ dTp), 3.96 (2 H, m, $H_{5'/5''}$ dTp), 4.01 (3 H, d, OCH_3, J = 11.6 Hz), 4.30 (1 H, m, $H_{4'}$ dTp), 4.36 (1 H, m, $H_{4'}$ pdC), 4.43 (1 H, m, $H_{5''}$ pdC), 4.50 (1 H, m, $H_{5'}$ pdC), 4.58 (1 H, m, $H_{3'}$ pdC), 5.02 (1 H, m, $H_{3'}$ dTp), 5.84 (1 H, d, H_5), 6.01 (1 H, m, $H_{1'}$ pdC), 6.03 (1 H, m, $H_{1'}$ dTp), 7.14 (1 H, s, H_6 dTp), 7.26 (1 H, d, H_6 pdC).

R_P Diastereoisomer (20 °C, 4.6 mM). ^{31}P NMR (D_2O): δ 2.10. ^{1}H NMR (D_2O): δ 2.38 (3 H, s, CH_3 base), 2.77 (1 H, m, $H_{2'}$ pdC), 2.84 (1 H, m, $H_{2'}$ dTp), 2.87 (1 H, m, $H_{2''}$ pdC), 2.97 (1 H, m, $H_{2''}$ dTp), 3.96 (2 H, m, $H_{5'/5''}$ dTp), 4.02 (3 H, d, OCH_3, J = 11.6 Hz), 4.31 (1 H, m, $H_{4'}$ dTp), 4.35 (1 H, m, $H_{4'}$ pdC), 4.42 (1 H, m, $H_{5''}$ pdC), 4.49 (1 H, m, $H_{5'}$ pdC), 4.59 (1 H, m, $H_{3'}$ pdC), 5.02 (1 H, m, $H_{3'}$ dTp), 5.87 (1 H, d, H_5), 6.02 (2 H, m, $H_{1'}$ pdC and dTp), 7.15 (1 H, s, H_6 dTp), 7.27 (1 H, d, H_6 pdC).

Registry No. (S_p)-**1**, 119185-00-1; (R_p)-**1**, 119241-90-6; (S_p)-**2**, 123808-83-3; (R_p)-**2**, 123808-84-4; (R_p)-d(T_6), 123751-57-5; (S_p)-d(T_6), 123808-85-5; (R_p)-d(C_6), 123751-58-6; (S_p)-d(C_6), 123808-86-6; thymidine, 50-89-5; 5′-*O*-(4-monomethoxytrityl)thymidine, 42926-80-7; 5′-*O*-(4-monomethoxyltrityl)thymidine-3′-phosphoramidate, 123751-59-7; 2′-deoxycytidine, 951-77-9; 5′-*O*-(4-monomethoxytrityl)dTpC, 123751-60-0.

Supplementary Material Available: ^{1}H NMR (600 MHz) spectra of phosphate-methylated R_P and S_P d(TpC) (4 pages). Ordering information is given on any current masthead page.

(26) van Genderen, M. H. P. Ph.D. Thesis, Eindhoven University of Technology, 1989.
(27) Haasnoot, C. A. G.; Hilbers, C. W. *Biopolymers* **1983**, *22*, 1259.
(28) Stec, W. J.; Zon, G.; Uznanski, B. *J. Chromatogr.* **1985**, *326*, 263.
(29) Schaller, H.; Weimann, G.; Lerch, B.; Khorana, H. G. *J. Am. Chem. Soc.* **1963**, *85*, 3821.
(30) Marugg, J. E.; Nielsen, J.; Dahl, O.; Burik, A.; van der Marel, G. A.; van Boom, J. H. *Recl. Trav. Chim. Pays-Bas* **1986**, *106*, 72.